Supplementary Information

Targeting CDK4/6 in glioblastoma via in situ injection of a cellulose-based hydrogel

Authors and affiliations:

[1,2]Xia Zhang[#], [3]Like Ning[#], [1]Hongshuai Wu[#], [1]Suisui Yang, [1]Ziyi Hu, [4]Wenhong Wang, [5]Yuandong Cao, [6]Hongliang Xin*, [3]Chaoqun You*, [1,7,8]Fan Lin*

[1] Department of Cell Biology, School of Basic Medical Sciences, Nanjing Medical University, Nanjing, Jiangsu, China

[2] Department of Central Laboratory, Shanghai Chest Hospital, Shanghai Jiao Tong University School of Medicine, Shanghai, China

[3] Jiangsu Key Lab for the Chemistry and Utilization of Agro-Forest Biomass, College of Chemical Engineering, Nanjing Forestry University, Nanjing, Jiangsu, China

[4] College of Pharmaceutical Science, Zhejiang University of Technology, Hangzhou, Zhejiang, China

[5] Department of Radiation Oncology, The First Affiliated Hospital of Nanjing Medical University, Nanjing, Jiangsu, China

[6] Department of Pharmaceutics, School of Pharmacy, Nanjing Medical University, Nanjing, Jiangsu, China

[7] Institute for Brain Tumors & Key Laboratory of Rare Metabolic Diseases, Nanjing Medical University; Nanjing, Jiangsu, China

[8] Department of Gastroenterology, The First Affiliated Hospital, and College of Clinical Medicine of Henan University of Science and Technology, Luoyang, Henan, China

[#] These authors contributed equally to this work.

*** Corresponding author:**

Fan Lin, PhD, E-mail: linfee@me.com

Hongliang Xin, PhD, E-mail: xhl@njmu.edu.cn

Chaoqun You, PhD, E-mail: chemyoucq@njfu.edu.cn

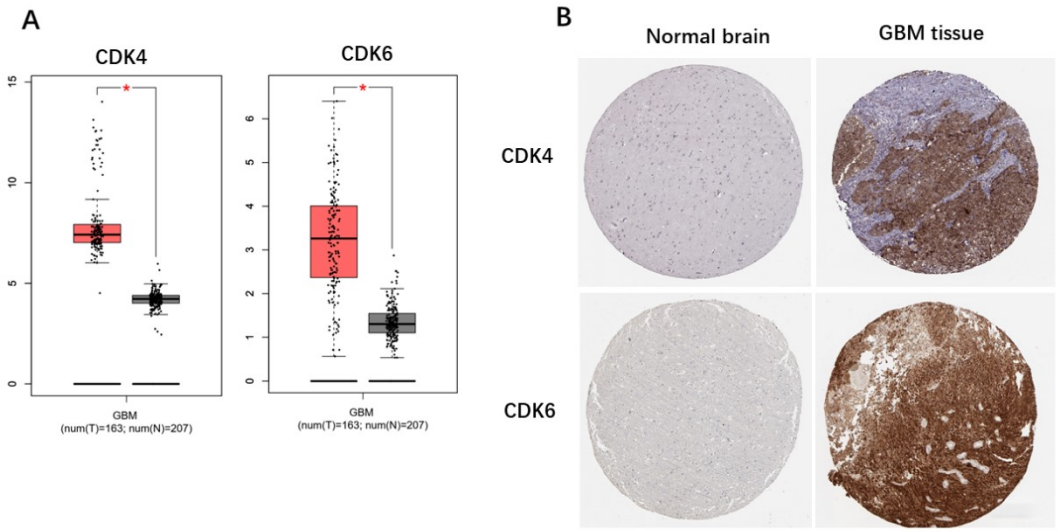

Figure S1. Expression levels of CDK4 and CDK6 are higher in GBM than normal brain tissue. (A) The comparison of mRNA levels of CDK4 and CDK6 in GBM tissues (n = 163) and normal brains (n = 207). (B) The immunohistochemical staining of CDK4 and CDK6 expression in GBM tissues and normal brains. The mRNA data were obtained from TCGA database and the graph in (A) were generated by GEPIA (http://gepia.cancer-pku.cn/). The protein staining of CDK4/6 of a representative example for each group were obtained from Protein Atlas (https://www.proteinatlas.org/).

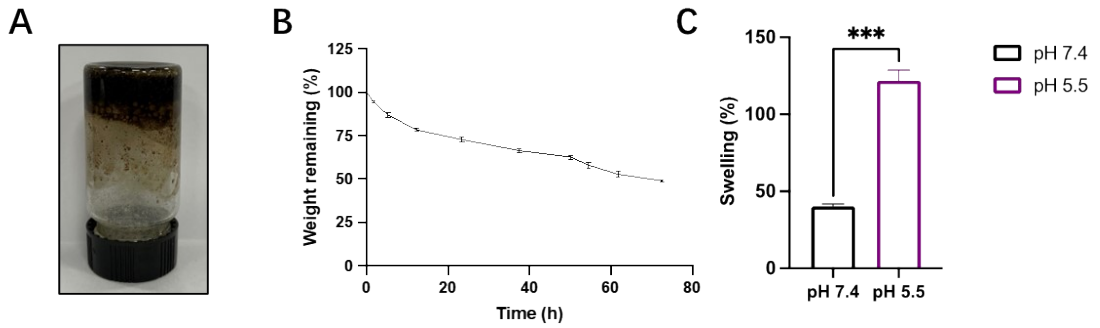

Figure S2. Additional characterization of PB@PH/Cu-CNCs hydrogel. (A) The outlook and inversion test of the PB@PH/Cu-CNCs hydrogel. (B) The degradation performance of the hydrogel at pH 7. (C) The mass swelling ratio of the hydrogel at different pH 5.5 and 7.4.

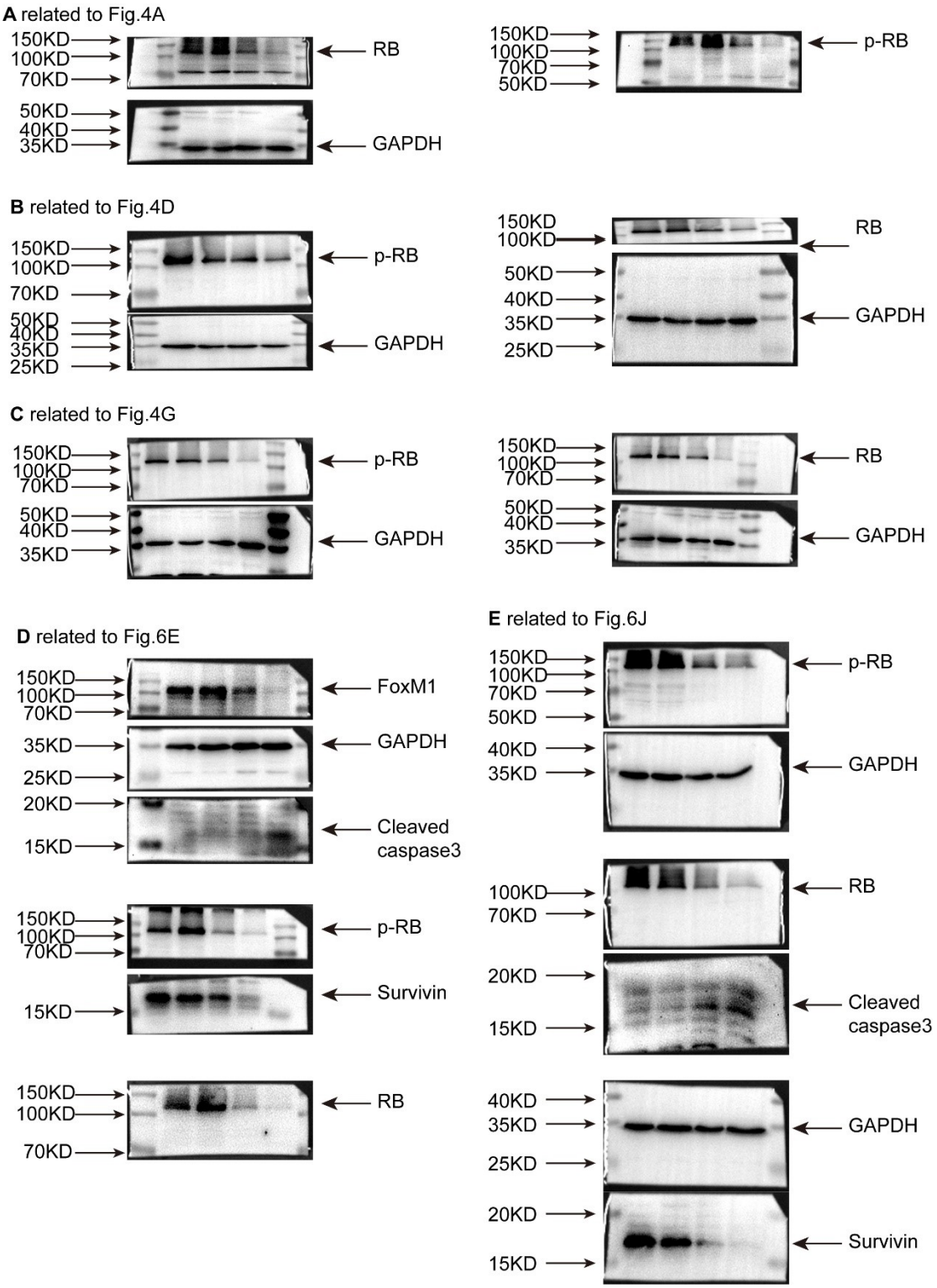

Figure S3. The uncropped images of the original Western blots. (A-E) Uncropped images of the original WB blots related to the representative WB blots shown in the Fig.4A, Fig.4D, Fig.4G, Fig.6E and Fig.6J.

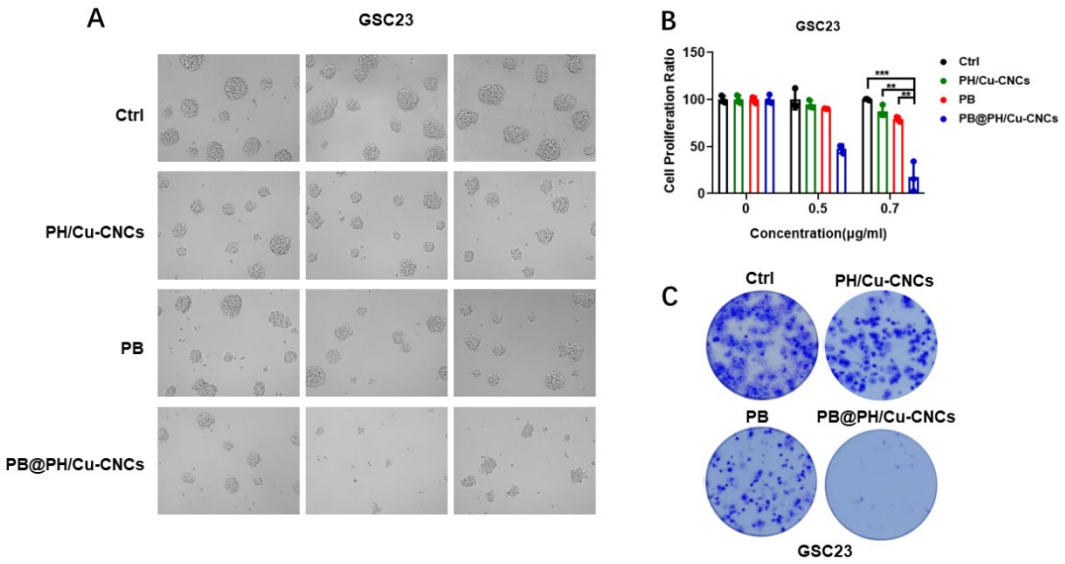

Figure S4. The growth inhibitory effect of PB@PH/Cu-CNCs in GSC (glioma stem cells). (A) The impact of PH/Cu-CNCs, free PB (0.1 μM) and PB@PH/Cu-CNCs treatment on the number and phenotype of neurosphere formed by GSC23 cells. (B) Quantification of neurospheres formed in each group in (A). **, $p < 0.01$; ***, $p < 0.001$. (C) Suppression of colony formation upon treatment with PH/Cu-CNCs, free PB and PB@PH/Cu-CNCs for 9-12 days in GSC23 cells.

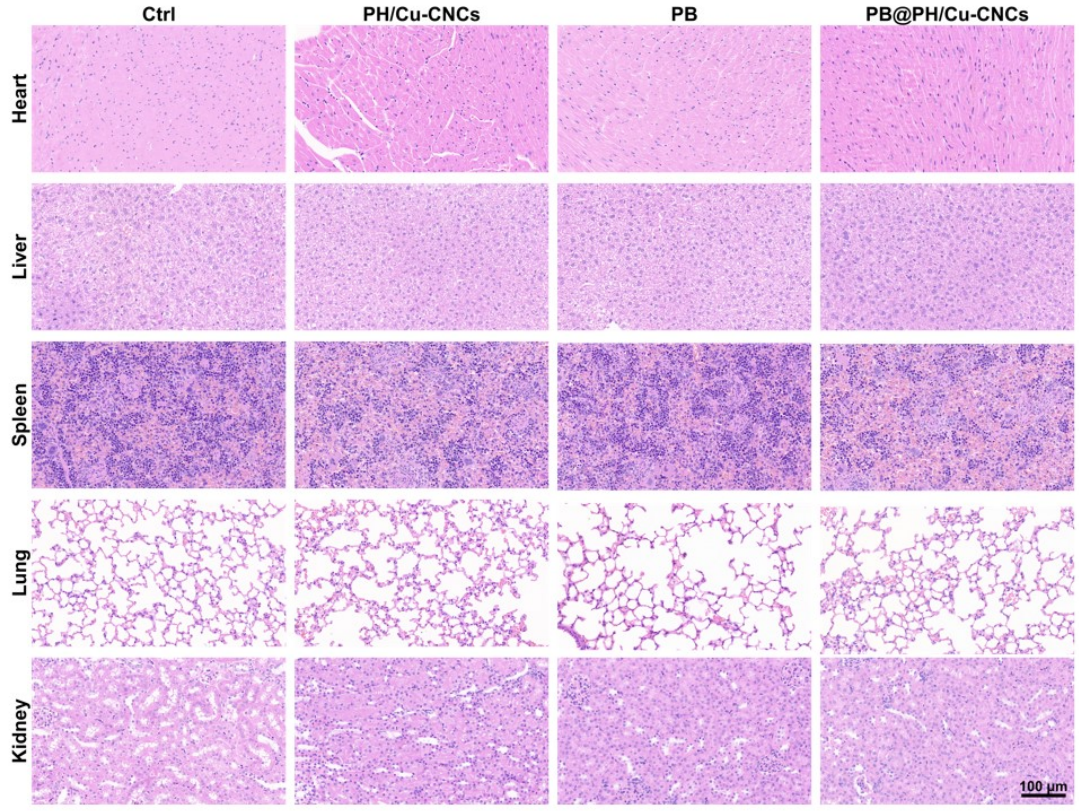

Figure S5. Evaluation of the in vivo toxicity of PB@PH/Cu-CNCs. H&E-stained tissue sections obtained from mice received intracranial injection of 10 μL PH/Cu-CNCs, free PB (3.84 mg/mL) or PB@PH/Cu-CNCs (30 mg/mL) for 7 days. Scale bar = 100 μm.